Human Molecular Genetics, 2007, Vol. 16, No. 3 ***265–275***
doi:10.1093/hmg/ddl454
Advance Access published on January 8, 2007

Functional characterization of GATA3 mutations causing the hypoparathyroidism-deafness-renal (HDR) dysplasia syndrome: insight into mechanisms of DNA binding by the GATA3 transcription factor

Asif Ali[1,†], Paul T. Christie[1,†], Irina V. Grigorieva[1,†], Brian Harding[1], Hilde Van Esch[2], S. Faisal Ahmed[3], Maria Bitner-Glindzicz[4], Eberhard Blind[5], Catherine Bloch[6], Patricia Christin[7], Peter Clayton[8], Jozef Gecz[9], Brigitte Gilbert-Dussardier[7], Encarna Guillen-Navarro[10], Anna Hackett[11], Isil Halac[12], Geoffrey N. Hendy[13], Fiona Lalloo[14], Christoph J. Mache[16], Zulf Mughal[15], Albert C.M. Ong[17], Choni Rinat[18], Nicholas Shaw[19], Sarah F. Smithson[20], John Tolmie[21], Jacques Weill[22], M. Andrew Nesbit[1] and Rajesh V. Thakker[1,*]

[1]Academic Endocrine Unit, Nuffield Department of Clinical Medicine, Oxford Centre for Diabetes, Endocrinology and Metabolism (OCDEM), University of Oxford, Churchill Hospital, Headington, Oxford OX3 7LJ, UK, [2]Department of Clinical Genetics, Centre for Human Genetics, University Hospital Leuven, Herestraat 49, B3000 Leuven, Belgium, [3]Royal Hospital for Sick Children, Dalnair Street, Glasgow G3 8SJ, UK, [4]Clinical and Molecular Genetics Unit, Institute for Child Health, London WC1 N1EH, UK, [5]Department of Medicine, Endocrinology, University of Würtzburg, Josef-Schneider-Str. 2, 97080 Würtzburg, Germany, [6]Hopital Lenval, 57 Av. De la Californie 06 200, Nice, France, [7]Service de Gènètique Mèdicale, CHU la Milètrie, B.P. 577, 86021 Poitiers-Cedex, France, [8]Royal Manchester Childrens Hospital, Hospital Road, Pendlebury, Manchester M27 4HA, UK, [9]Department of Genetic Medicine, Women's and Children's Hospital, 72 King William Road, North Adelaide, SA 5006, Adelaide, Australia, [10]Unidad de Genetica Medica, Hospital Universitario Virgen de la Arraxaca, Ctra Madrid-Cartagena, El Palmar 30120, Spain, [11]Hunter Genetics, PO Box 84, Waratah, New South Wales 2298, Australia, [12]Children's Memorial Hospital, 2300 Children's Plaza, Chicago, ILL 60614-3394, USA, [13]Calcium Research Laboratory, Royal Victoria Hospital, 687 Pine Av. West, Montreal, Quebec H3A 1A1, Canada, [14]Department of Clinical Genetics, [15]Department of Paediatrics, Saint Mary's Hospital for Women and Children, Hathersage Road, Manchester M13 OJH, UK, [16]Department of Paediatrics Medical University, Graz, Auenbruggerplatz 30, A-8036 Graz, Austria, [17]Academic Nephrology Unit, Sheffield Kidney Institute, University of Sheffield, Northern General Hospital, Herries Road, Sheffield S5 7AU, UK, [18]Pediatric Nephrology Unit, Shaare Zedek Medical Centre, POB 3235, Jerusalem, Israel, [19]Birmingham Children's Hospital, Steelhouse Lane, Birmingham B4 6NH, UK, [20]Department of Clinical Genetics, St Michael's Hospital, Bristol BS2 8EG, UK, [21]Institute of Medical Genetics, Yorkhill NHS Trust, Dalnair Street, Glasgow G3 8SJ, UK and [22]Pediatric Endocrine Unit, University Hospital, Lille, France

Received October 18, 2006; Revised and Accepted November 30, 2006

*To whom correspondence should be addressed. Tel: +44 1865857501; Fax: +44 1865857502; Email: rajesh.thakker@ndm.ox.ac.uk
[†]The authors wish it to be known that, in their opinion, the first three authors should be regarded as joint First Authors.

The hypoparathyroidism-deafness-renal (HDR) dysplasia syndrome is an autosomal dominant disorder caused by mutations of the dual zinc finger transcription factor, GATA3. We investigated 21 HDR probands and 14 patients with isolated hypoparathyroidism for *GATA3* abnormalities. Thirteen different heterozygous germline mutations were identified in patients with HDR. These consisted of three nonsense mutations, six frameshifting deletions, two frameshifting insertions, one missense (Leu348Arg) mutation and one acceptor splice site mutation. The splice site mutation was demonstrated to cause a pre-mRNA processing abnormality leading to the use of an alternative acceptor site 8 bp downstream of the normal site, resulting in a frameshift and prematurely terminated protein. Electrophoretic mobility shift assays (EMSAs) revealed three classes of GATA3 mutations: those that lead to a loss of DNA binding which represent over 90% of all mutations, and involved a loss of the carboxy-terminal zinc finger; those that resulted in a reduced DNA-binding affinity; and those (e.g. Leu348Arg) that did not alter DNA binding or the affinity but likely altered the conformational change that occurs during binding in the DNA major groove as predicted by a three-dimensional modeling. These results elucidate further the molecular mechanisms underlying the altered functions of mutants of this zinc finger transcription factor and their role in causing this developmental anomaly. No mutations were identified in patients with isolated hypoparathyroidism, thereby indicating that GATA3 abnormalities are more likely to result in two or more of the phenotypic features of the HDR syndrome and not in one, such as isolated hypoparathyroidism.

INTRODUCTION

Inherited forms of hypoparathyroidism may occur as either isolated endocrinopathies with autosomal dominant, autosomal recessive or X-linked recessive transmission, or as part of complex congenital anomalies such as the DiGeorge (MIM no. 188400) (1), Kenny–Caffey (MIM no. 244460) and hypoparathyroidism-deafness-renal (HDR) dysplasia (MIM no. 146255) syndromes (http://www.ncbi.nlm.nih.gov/entrez/query.fcgi?db=OMIM) (1–8). The DiGeorge syndrome, which is characterized by parathyroid hypoplasia, thymic hypoplasia, T-cell mediated immunodeficiency, and cardiac defects, is due to deletions of chromosome 22q11.2 that encompass abnormalities of the T-box transcription factor-1 (*TBX1*) gene (8,9). The Kenny–Caffey syndrome, which is characterized by hypoparathyroidism, short stature, osteosclerosis, cortical thickening of long bones and eye abnormalities, is associated with mutations of the Tubulin-binding chaperone-E (*TBCE*) gene that is located on chromosome 1q42.3 (5,10). The HDR syndrome, an autosomal dominant disorder, is caused by mutations of the *GATA3* gene that is located on chromosome 10p15 (3). GATA3 belongs to a family of dual zinc finger transcription factors that are involved in vertebrate embryonic development. The six mammalian GATA proteins (GATA 1 to 6) share related Cys-X_2-Cys-X_{17}-Cys-X_2-Cys (where X represents any amino acid residue) zinc finger DNA-binding domains and bind to the consensus motif 5′-(A/T)GATA(A/G)-3′ (11). The C-terminal finger (ZnF2) is essential for DNA binding, whereas the N-terminal finger (ZnF1) helps stabilize this binding and to physically interact with other proteins such as the multi-type zinc finger Friends of GATA (FOG) (11–13). The importance of these dual functions of the two zinc fingers has been well illustrated by studies of *GATA3* mutations associated with the HDR syndrome. Thus, of the 25 HDR causing *GATA3* mutations (Fig. 1) reported to date, six are whole gene losses, 10 are mutations that disrupt ZnF2 and lead to a loss of DNA binding, two are mutations that disrupt ZnF1and destabilize DNA binding and/or its interaction with FOG2 and seven are deletions/insertions that disrupt both ZnF1 and ZnF2 (3,6,7,13–18). To gain further insights into the role of GATA3 mutations in causing the HDR syndrome, we have studied additional HDR patients for GATA3 abnormalities.

RESULTS

GATA3 mutations

DNA sequence analysis of the entire 1332 bp coding region together with the associated splice sites, and 5′ and 3′ untranslated regions of the *GATA3* gene from each of the 21 probands with HDR (Table 1) revealed the presence of 13 different heterozygous mutations; 11 of these mutations are novel and two, an intragenic insertion at codon 135 and a nonsense mutation at codon 277, have been previously identified (3,17) in unrelated families (Fig. 1 and Table 2). Thus, three of the mutations were nonsense mutations, six were frameshifting deletions, two were frameshifting insertions, one was a missense mutation (Fig. 2) and one was an acceptor splice site mutation (Fig. 3). The occurrence of the three nonsense mutations (Gln22Stop, Gly248Stop and Arg277Stop), two of the frameshifting mutations, which involved codons 144 and 407, and the missense mutation (Leu348Arg) were confirmed by restriction endonuclease analysis (Fig. 2 and Table 2). The occurrences of the remaining seven mutations, which were not associated with altered restriction endonuclease sites, were confirmed by repeat DNA sequence analyses. The absence of all of these DNA sequence abnormalities in 110 alleles from 55 unrelated normal individuals indicated that these 13 abnormalities were mutations and not functionally neutral polymorphisms that would be expected to occur in $>1\%$ of the population. The missense mutation (Leu348Arg), which was detected in the proband from family 8.2/04

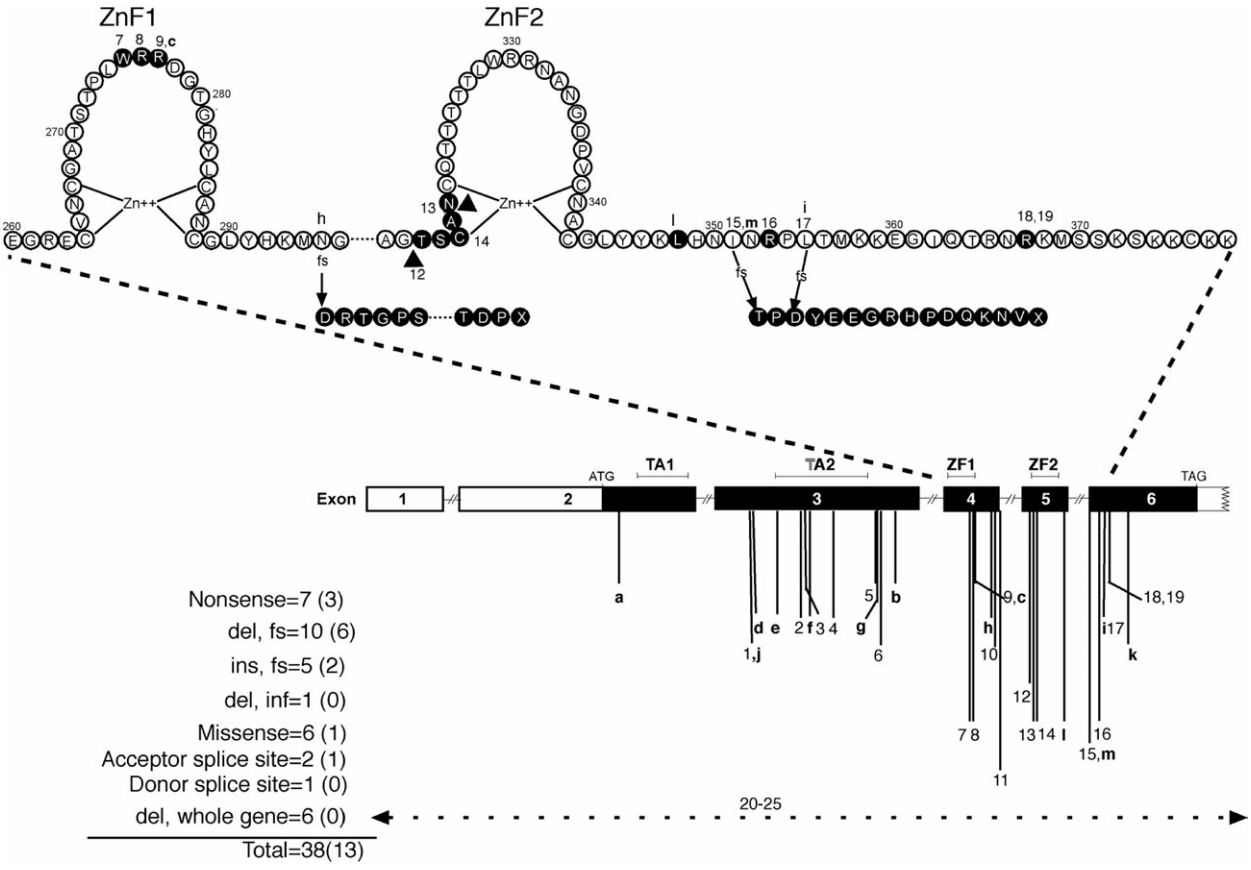

Figure 1. Schematic representation of the genomic structure of the *GATA3* gene illustrating the locations of mutations identified in HDR patients. The human *GATA3* gene consists of six exons, spanning 20 kb of genomic DNA and encodes a 444-amino acid transcription factor that contains two transactivating domains (TA1 and TA2) and two zinc fingers (ZnF1 and ZnF2). The sizes of exons 1, 2, 3, 4, 5 and 6 are 188, 610, 537, 146, 126 and 806 bp, respectively. The ATG (translation start) and the TAG (Stop) sites are in exons 2 and 6, respectively. The locations of the 13 HDR mutations identified by the present study are shown (letters a to m) which correspond to the mutations detailed in Table 2, together with 19 previously reported mutations numbered 1 to 19 (3,13–18). In addition, six whole gene deletions (del) have been previously reported (3,14). This yields a total of 38 GATA3 abnormalities in HDR patients. Sixteen of the 38 HDR mutations, which affect the region encompassing the two zinc fingers and the adjacent C-terminal region, are further detailed above in the amino acid sequence, in which every tenth amino acid is numbered. The amino acids altered by the 16 HDR mutations are highlighted in black. fs, frameshift; inf, inframe.

(Table 2), was demonstrated to be absent in both parents and was hence found to be arising *de novo* (Fig. 2). This novel Leu348Arg mutation involves a residue that is evolutionary conserved in man, mouse, rat and zebrafish (Ensembl database; www.ensembl.org, www.ebi.ac.uk/clustalw/) and is thus likely to be of significance. None of the 14 patients with isolated hypoparathyroidism was found to harbor *GATA3* mutations.

All of the 13 *GATA3* mutations, which occurred in exons 2–6 (Fig. 1), predict structurally significant changes (Table 2). Thus, the three nonsense mutations Gln22Stop, Gly248Stop and Arg277Stop, the five frameshift deletions occurring in codons 135, 144, 164, 236 and 295/296 and the frameshift insertion occurring at codon 135 are predicted, if translated, to have truncated GATA3 proteins that lack both ZnFs. These mutations are likely to result in a loss of DNA binding, as has been demonstrated for other such *GATA3* mutations (13,19). The frameshift deletion occurring in codon 355 is predicted to lead to a truncated GATA3 protein that lacks the C-terminal region adjacent to ZnF2. These mutations are also likely to result in a loss of DNA binding, as has been demonstrated for other such *GATA3* mutations, e.g. Arg367Stop, and a frameshift deletion involving codon 355 (13). However, the effects of: the missense mutation Leu348Arg which involves substitution of a highly conserved, neutral hydrophobic amino acid leucine for a basic, hydrophilic residue arginine; the frameshift insertion occurring in codon 407 (407 ins C) which predicts the occurrence of 98 missense residues and hence an elongated protein of 506 amino acids; and of the mutation involving the invariant *ag* dinucleotide of the consensus acceptor splice site at the intron 5/exon 6 boundary, are more difficult to predict and these were investigated further.

mRNA splicing abnormality due to acceptor splice site mutation

The acceptor splice site mutation is likely to result in abnormal processing of mRNA, and we investigated this using total RNA obtained from Epstein-Barr virus (EBV)-transformed lymphoblastoid cell lines that had been established from the HDR patient of family 8/05 (Table 2) and an unrelated normal individual. The *a* nucleotide at position −2 together with the

Table 1. Clinical and biochemical findings in 29 HDR patients in 21 families

Mutation[a]	Family/patient/sex[b]	Hypoparathyroidism		Presentation[d]	Age[e]	Deafness (sensorineural)		Renal abnormalities[g], age[e]
		Serum Ca^{2+} mmol/L[c]	Serum PTH pg/ml			Symmetry[f]	Age[e]	
a	20/04 Proband M	2.05	6	As	5 year	B	2 year	None
	Mother F	L	L	As	Adult	B	Adult	MGPN, renal insufficiency
b	22/04 Proband F	2.10	3	Se, Te	2 days	B	5 year	C
c	7/05 Proband F	1.04	<6	Se	33 year	B	Child	H, ESRF
d	4/04 Proband F	1.70	L	Te	31 year	B	13 year	None
e	2/04 Proband M	1.39	9	Se	4 year	B	6 year	A, 4 year
f	3.1/04 Proband F	L	L	Se	Neonate	B	10 month	None
g	8/04 Proband F	1.25	3	Te	35 year	L > R	3	C, H, 36 year
	Daughter F	L	19	As	14 year	B	2.5 year	None
	Son M	L	8	As	7 year	B	Birth	None
h	3/04 Proband M	2.13	7	Se	6 year	B	5 year	H, S, 10 year
	Sister F	2.15	14	As	1 year	B	7 year	H, S, VR, 1 year
	Mother F	2.14	18	Te	Adult	B	38 year	H, S, VR, Adult
i	14/05 Proband M	1.72	<5	Se	8 month	B	1 year	H, 8 month
j	13/05 Proband F	2.03	5	As	8 month	B	3 year	D, VR, 8 month
	Father M	1.63	9	As	25 year	B	7 year	A, D, ESRF, 25 year
	Sister F	0.84	<5	As	8 year	B	8 year	VR, 10 month
k	16/05 Proband F	2.05	L	Se	1 month	B	Birth	H, *in utero*
l	8.2/04 Proband M	1.69	<1	Se, LQ	14 year	R > L	Birth	None
m	8/05 Proband F	1.51	1.3 pM ($N = 0.8$-7.7)	Te	2 month	B	2 month	D, VR, S, 1 year
NF	2/05 Proband F	1.55	5	Se, Te	6 month	B	3.25 year	D, VR, 9 month
NF	7/03 Proband M	1.39	1.1pM ($N = 0.8$-7.7)	Se, Te	3 weeks	L > R	4 year	None
NF	2/03 Proband F	1.18	<10	Se, Te	7.5 year	B	Child	None
NF	23/05 Proband M	1.58	15	Se	2 year	B	Child	None
NF	2.1/04 Proband F	2.11	0.5 pM ($N = 1.1$-5.4)	As	7 year	B	5.5 year	None
NF	3.2/04 Proband F	L	L	N/A	Early	N/A	10 month	None
NF	6/05 Proband M	1.92	8	Te	Neonate	B	6 month	None
NF	Mother F	L	11	Te	24 year	None		None
NF	2.1/03 Proband F	1.68	0.6 pM ($N = 0.8$-7.7)	As	Neonate	B	2 year	None
	Normal range:	2.20–2.65	10–55					

[a]Mutation location and details are shown in Figure 1 and Table 2, respectively. NF, mutation within coding region and splice sites not found.
[b]Sex: M, male; F, female.
[c]L: low, exact value not known, serum Ca^{2+}-pretreatment values. N/A denotes details not available.
[d]As, asymptomatic; Se, seizures; Te, tetany; LQ, long Q interval.
[e]Age of onset/diagnosis.
[f]Deafness: B, bilateral; S, symmetrical; R, right ear; L, left ear.
[g]Renal abnormalities: D, dysplasia; H, hypoplasia; A, aplasia; C, cysts; S, sepsis; ESRF, end-stage renal failure; MPGN, mesangioproliferative glomerulonephritis; VR, vesicouteric reflux.

g nucleotide at position −1, of the acceptor splice consensus sequence are invariant in eukaryotic sequences (20) and mutations involving these invariant sequences have been previously reported (13,21,22). Such studies have revealed that mutations in the acceptor splice site regions may be associated with an accumulation of unspliced precursor mRNA, retention of incompletely spliced precursors, complete absence of transcripts or the appearance of aberrantly processed mRNA from the use of alternative normally occurring splice sites or cryptic splice sites (13,21–24). To investigate these possibilities, we examined *GATA3* mRNA processing by the detection of its transcription in EBV-transformed lymphoblastoid cell lines (Fig. 3). This revealed, in addition to the wild-type product, the presence of an aberrantly processed mRNA. DNA sequence analysis of the mutant *GATA3* product revealed that the mutation had lead to utilization of an alternative acceptor splice site that had resulted in a loss of 8 nucleotides from the mRNA. This would lead to a frameshift that, if translated, would produce a missense peptide with a termination at codon 367. This abnormality of mRNA processing, which results from a mutation at position −2 of the acceptor splice site consensus sequence, is identical to that associated with another HDR mutation in which there was a *g* to *t* transversion involving position −1 of the same acceptor splice site (13). Moreover, these two studies utilized different methods to demonstrate the mRNA processing abnormalities. Thus, the present study investigated for endogenous *GATA3* transcription in EBV-transformed lymphoblastoid cell lines from an HDR patient and a normal individual (Fig. 3), whereas the previous study (13) investigated for *GATA3* transcription in COS-1 cells that had been transiently transfected with either wild-type or mutant mini-*GATA3* gene constructs. Both of these independent

Table 2. GATA3 abnormalities detected in HDR patients

Mutation[a]	Family/patient[b]	Exon	Codon	Base change	Amino acid change	RE/SA[c]	Predicted effect[d]
Nonsense mutations							
a	20/04	2	22	**C**AG → **T**AG	Gln → Stop	RE	Q22X Loss of ZnF1 and ZnF2; HI
b	22/04	3	248	**G**GA → **T**GA	Gly → Stop	RE	G248X Loss of Znf1 and ZnF2; HI
c[e]	7/05	4	277	**C**GA → **T**GA	Arg → Stop	RE	R277X Loss of Znf1 and ZnF2; HI
Intragenic deletions (Δ)							
d	4/04	3	135	**C**CG → -CG	Frameshift	SA	Missense peptide 59 amino acids from 136 to 193, followed by premature stop at codon 194: truncated protein with loss of ZnF1 and ZnF2; HI
e	2/04	3	144	G**G**C → G-C	Frameshift	RE	Missense peptide 50 amino acids from 145 to 193, followed by premature stop at codon 194; truncated protein with loss of ZnF1 and ZnF2; HI
f	3.1/04	3	164	**G**AC → -AC	Frameshift	SA	Missense peptide 29 amino acids from 165 to 193, followed by premature stop at codon 194: truncated protein with loss of ZnF1 and ZnF2; HI
g	8/04	3	236	CC**C** → CC-	Frameshift	SA	Missense peptide 28 amino acids from 237 to 264, followed by premature stop at codon 265: truncated protein with loss of ZnF1 and ZnF2; HI
h	3/04	4	295–6	**AAC G**GA → -GA	Frameshift	SA	Missense peptide 59 amino acids from 296 to 354, followed by premature stop at codon 355: truncated protein with loss of ZnF1 and ZnF2; HI
i[f]	14/05	6	355	C**T**G → C-G	Frameshift	SA	Missense peptide 1 amino acid at 356, followed by premature stop at codon 357: truncated protein with loss of ZnF2; HI
Intragenic insertions							
j[g]	13/05	3	135	CCG → CC**C**G	Frameshift	SA	Missense peptide 165 amino acids from 136 to 301, followed by premature stop at codon 302: truncated protein with loss of ZnF2; HI
k[f]	16/05	6	407	ATC → ATC**C**	Frameshift	RE	Missense peptide 98 amino acids from 408 to 506, followed by stop at codon 507 in new frame: loss of basic amino acids flanking ZnF2, HI

Continued

Table 2. *Continued.*

Mutation[a]	Family/patient[b]	Exon	Codon	Base change	Amino acid change	RE/SA[c]	Predicted effect[d]
Missense mutation l[f]	8.2/04	5	348	C**T**T → C**G**T	Leu → Arg	RE	L348R; Affects basic region. Likely to affect DNA conformational change
Splice-site mutation m[f]	8/05	Intron5/exon 6 boundary	Nucl 1250-2	**a**g → **g**g	Frameshift	SA	Missense peptide, 18 amino acids followed by premature stop at codon 367. Loss of basic amino acids flanking ZnF2, HI

[a]Mutation letter refers to location shown in Figure 1.
[b]Family identification refers to clinical details shown in Table 1.
[c]Analysis by restriction enzymes (RE), or sequence analysis (SA).
[d]Haploinsufficiency (HI).
[e]Identified previously in an unrelated family (3).
[f]*De novo* mutation not present in either parent of proband.
[g]Identified previously in an unrelated family (17).

methods demonstrated that the two different mutations of the intron 5/exon 6 acceptor splice site, lead to utilization of the normally occurring, but non-utilized, alternative acceptor splice site at codons 351–353, with a resulting frameshift and prematurely terminated GATA3 peptide. Thus, these results indicate that the *GATA3* sequence at codons 351–353 comprises a strong acceptor splice site consensus that may be utilized if the upstream acceptor splice site is disrupted.

DNA-binding studies of Leu348Arg and 407 ins C GATA3 mutants

The Leu348Arg mutation is located 6 residues away from ZnF2 (Fig. 1) and the 407 ins C does not disrupt ZnF2 or its adjacent C-terminal basic region. As the previously reported nonsense mutation, Arg367Stop, and two frameshift mutations involving codons 351 and 355 have been shown to lead to a loss of DNA binding (13), we decided to investigate these two GATA3 mutations for alterations in DNA binding by the use of EMSA. The Leu348Arg and 407 ins C GATA mutants were initially assessed for altered DNA binding by EMSAs (Fig. 4), using nuclear extracts from COS-7 cells transfected with either wild-type or mutant *GATA3* constructs. This revealed that the 407 ins C mutation resulted in a loss of DNA binding, but that the Leu348Arg mutant retained DNA binding (Fig. 4), despite being in close proximity to ZnF2 (Fig. 1). It is also interesting to note that the expression of the 407 ins C GATA3 mutant protein was markedly reduced when compared with that of the wild-type (Fig. 4) and this suggests that the larger mutant GATA3 protein may be less stable. This is in agreement with previous studies (25) of GATA1 mutant proteins, which have been shown not to accumulate *in vitro* to the levels observed for wild-type proteins. Indeed some GATA1 deletions appeared to be associated with increased sensitivity of the translated protein to endogenous proteases. These results are also in agreement with other studies of GATA1 binding (25,26) which showed that ZnF2 peptides truncated at Arg298 and Thr304 (equivalent to GATA3 Lys358 and Thr364) lost DNA binding, whereas a peptide truncated at Ser310 (equivalent to GATA3 Ser370) retained DNA binding. Within this interval lies a conserved QTRNRK motif (Fig. 5), which is located in the minor groove and is important for DNA binding. Although this QTRNRK motif is retained in the 407 ins C mutant GATA3 protein, it nevertheless seems possible that the large C-terminal extension in this mutant GATA3 protein may sterically interfere with DNA binding. Thus, a loss of DNA binding together with a decreased stability of the mutant GATA3 protein is likely to be contributing to the haploinsufficiency causing HDR in this patient with the 407 ins C mutation.

The Leu348Arg GATA3 mutant was further assessed for alterations in the affinity of DNA binding by utilizing a dissociation EMSA. This revealed that the Leu348Arg GATA3 mutant had the same DNA-binding affinity as the wild-type GATA3 protein. The addition of GATA3 antibody to the reaction mix resulted in the detection of a higher molecular weight band, thereby confirming the presence of GATA3 protein in the complex (Fig. 4). Thus, these results indicate that the Leu348Arg GATA3 which occurs in an HDR patient (Fig. 2), is not associated with altered DNA binding or a change in the affinity of DNA binding.

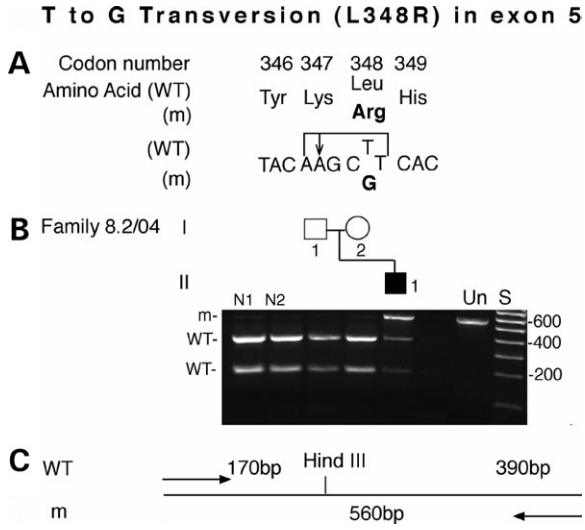

Figure 2. Detection of *GATA3* mutation in exon 5 in family 8.2/04 with HDR by restriction enzyme analysis (**A**), DNA sequence analysis of individual II.1 revealed a **T** to **G** transversion at codon 348, thus altering the wild-type (WT) sequence C**T**T, encoding a leucine (Leu, L) to the mutant (m) sequence C**G**T, encoding an arginine (Arg, R). (**B**), The missense mutation also resulted in the loss of the wild-type *Hind III* restriction enzyme (A/AGCTT), and this facilitated the confirmation of the mutation. (**C**), PCR amplification and *Hind III* digestion would result in two products of 170 and 390 bp from the normal (WT) sequence as illustrated in the restriction map. The affected individual, II.1 was shown to be heterozygous for the mutation, and the absence of this Leu348Arg mutation in 110 alleles from 55 unrelated normal individuals (N1 and N2 shown) indicates that it is not a common DNA sequence polymorphism. Furthermore, the absence of this Leu348Arg mutation in both of the unaffected parents indicates that the mutation arose *de novo* in the proband, II.1. Individuals are represented as male (square), female (circle), unaffected (open symbols) and affected (filled symbols). Un-undigested DNA, S- DNA size markers are from a 100 bp ladder.

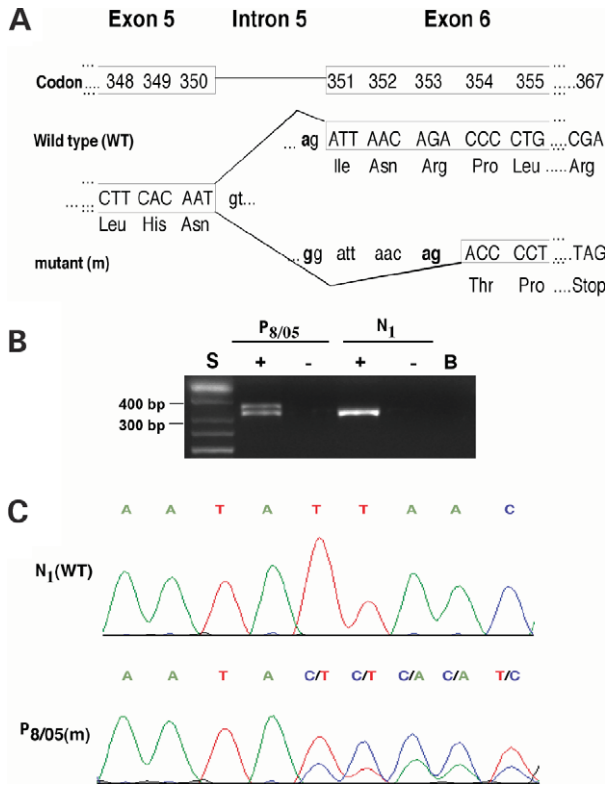

Figure 3. Detection of acceptor splice site mutation at the intron 5/exon 6 boundary in proband 8/05 with HDR. (**A**), DNA sequence analysis of the affected proband (Tables 1 and 2) revealed an *a* to *g* transition at the −2 position, which resulted in an alteration of the invariant *ag* acceptor splice site. Analysis of 110 alleles from 55 unrelated normal individuals revealed the presence of the normal *ag* acceptor splice site and an absence of the *gg* sequence thereby indicating that the *a* to *g* transition at position −2 was not a common sequence polymorphism (data not shown) but a likely mutation that would alter mRNA splicing. In addition, an examination of the DNA sequences of codons 351–353 revealed another naturally occurring, but normally unused acceptor splice site sequence (*ncag*) (24,40). Exonic sequence (upper case) and intronic sequence (lower case). (**B**) The effects of the likely mutation were investigated by RT–PCR, using RNA obtained from EBV-transformed lymphoblastoids of the proband ($P_{8/05}$) and a normal subject (N_1). Only one RT–PCR product (342 bp) was obtained from the normal individual, but two products (342 and 334 bp) were obtained from the HDR patient. The positions of the size markers (S, 100 bp ladder) are indicated. +, with AMV reverse transcriptase; −, without AMV reverse transcriptase; B, control water blank, i.e. no RNA used. (**C**) DNA sequence analyses of the RT–PCR products confirmed correct splicing in the normal (WT) individual and revealed that the mutation at position −2 of the acceptor splice site in $P_{8/05}$ lead to splicing of exon 5 to an internal site in exon 6 that resulted in a new sequence, which encoded a missense peptide with a premature termination at codon 367. Thus, the mutation resulted in utilization of an alternative, naturally occurring, but normally non-utilized, acceptor splice site sequence.

HDR phenotypes and GATA3 mutations

GATA3 mutations were found in 20 of the 29 HDR patients (Tables 1 and 2) but in none of the 14 patients with isolated hypoparathyroidism. The results of this study were pooled with those of our three previous studies (3,13,15), from which detailed clinical data were available for an analysis of the phenotypes associated with *GATA3* mutations. This yielded data from 63 individuals that consisted of 40 with *GATA3* mutations and 23 without *GATA3* mutations (Table 3). This revealed that >90% of patients with the three cardinal clinical features of the HDR syndrome had *GATA3* mutations, but that <65% of patients with hypoparathyroidism and deafness had *GATA3* mutations (Table 3). None of the 14 patients with isolated hypoparathyroidism had *GATA3* mutations. These results indicate that *GATA3* mutations are most likely to result in patients having two or three of the phenotypic manifestations of HDR, but not in isolated hypoparathyroidism.

DISCUSSION

Our results, which have identified 13 different mutations of the *GATA3* gene (Table 2) in 13 of the 21 probands and their families, expand the spectrum of mutations and help further establish the role of GATA3 haploinsufficiency in the aetiology of this developmental disorder. However, it is important to note that such *GATA3* mutations involving the coding region and adjacent splice sites were not detected in eight of the 21 probands (Tables 1 and 2). It remains possible that these patients may harbor mutations in the regulatory sequences flanking the *GATA3* gene, or involve deletions of the whole gene or complete exons, or else they may represent genetic heterogeneity. Moreover, it is interesting to note that seven of these eight patients do not have renal abnormalities, and it thus seems likely that *GATA3* mutations are likely to be

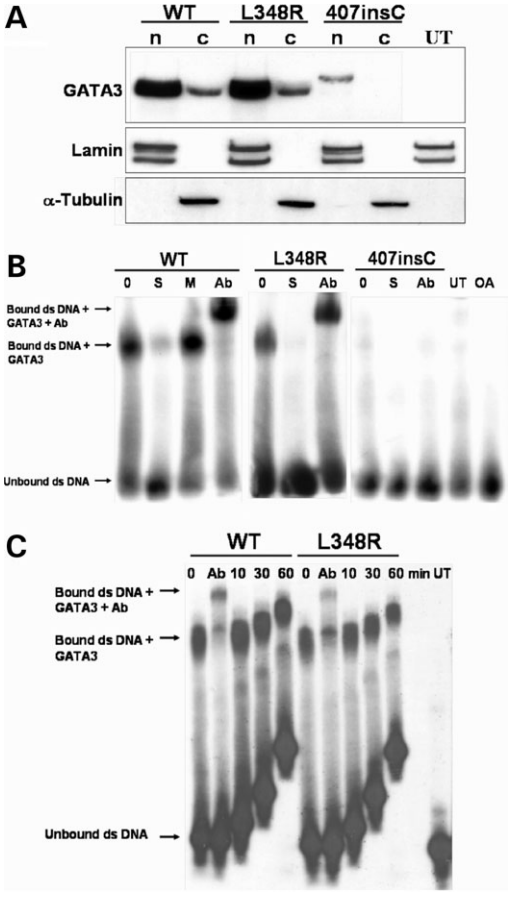

Figure 4. Analysis of DNA-binding properties and subcellular localization of Leu348Arg (L348R) and 407ins C GATA3 mutant proteins. (**A**), Western blot analysis of nuclear and cytoplasmic extracts from COS-7 cells transfected with either the wild-type (WT) or mutant GATA3 (L348R or 407ins C) constructs. This revealed that the WT and mutant GATA3 proteins were predominantly located in the nucleus. The expected 49 kDa WT and L348R GATA3 proteins were observed, while the 407ins C mutation was found to result in a protein with a higher molecular mass of 55 kDa and consistent with it being an elongated missense peptide of 506 residues. Antibodies against the nuclear protein lamin, and cytoplasmic protein α-tubulin, were used to assess the quality of subcellular preparations. (**B**), DNA binding of mutant GATA3 proteins was assessed using EMSA where nuclear extracts were incubated with a radiolabeled (^{32}P) double-stranded oligonucleotide containing the GATA consensus DNA sequence. Control binding reactions using untransfected (UT) cells and the oligonucleotide alone (OA), i.e. without nuclear extract, were performed. The WT GATA3 bound to double-stranded (ds) DNA and the specificity of binding to the GATA motif was confirmed with competition in the presence of 100-fold excess of unlabeled specific oligo (S) or mutant oligo (M) in which the GATA site was abolished. Supershift assay with GATA3 antibody (Ab) further confirmed the presence of GATA3 in the protein-DNA complex. The L348R mutant bound to DNA, while the 407ins C mutant resulted in a loss of DNA binding. (**C**), The stability of DNA binding of the L348R mutant was studied using a dissociation shift assay in which unlabeled dsDNA was added and the effect on binding of GATA3 to the radiolabeled dsDNA measured over a time course of 60 min by autoradiography. The L348R mutant dissociated from DNA at the same rate as WT protein indicating that the mutation does not affect the stability of binding to DNA.

highly penetrant and result in phenotypic manifestations involving the parathyroids, kidneys and hearing loss (Table 3). This would be consistent with the decreased frequency of such mutations in patients with involvement of two of the three organs and with the absence of *GATA3* mutations in patients with isolated hypoparathyroidism. We did not undertake similar studies in patients with non-syndromic deafness or isolated renal dysplasia as these disorders are common and have been reported to be due to mutations in several genes that include GJB2/connexin 26 (27,28), and PAX2 and Uroplakin III (29,30), respectively. Thus, our analysis indicates that in the clinical setting, a search for *GATA3* mutations would be worthwhile mainly in patients with either two or three, of the phenotypic manifestations of the HDR syndrome, but not in those with only one of the clinical features.

The majority, i.e. >90% of the 13 *GATA3* mutations (Table 2) identified by this study are predicted to result in truncated forms of the protein, and this is consistent with the findings of previous studies (3,13,14). Indeed, of the total of 38 *GATA3* mutations reported to date (Fig. 1), 65% are truncating mutations (i.e. nonsense, frameshift deletions, frameshift insertions, or involving a splice site), 16% are gene deletions, 3% involve an in-frame deletion and 16% are missense mutations. These *GATA3* mutations can also be divided broadly into three classes, based upon their functional consequences with respect to alterations in DNA binding. The first class is represented by those mutations that lead to a loss of DNA binding, and this contains the majority (92%) of mutations that result in truncated or deleted forms of GATA3 which lack ZnF2 (Fig. 1) (3,13,14,16–18). The codon 407 ins C, although it contains ZnF2, would also belong to this class as it results in a loss of DNA binding (Fig. 4). The second class is defined by a loss of DNA-binding affinity, and is represented by one HDR associated missense mutation, Arg276Pro (15). This mutant GATA3 which involves ZnF1, binds to DNA, but with a reduced affinity such that it rapidly dissociates from the bound DNA when compared with the wild-type GATA3 (15). The third class is characterized by normal DNA binding with normal affinity and is represented by two HDR associated missense mutations, Trp275Arg and Leu348Arg (Figs 2 and 4). The Trp275Arg involves ZnF1 and leads to a loss of interaction with FOG2 (13), whereas the Leu348Arg mutation identified in this study (Fig. 2) does not involve ZnF1 or ZnF2 but instead is located six residues, in the C-terminal direction, away from ZnF2 (Figs 1 and 5). This Leu348Arg *GATA3* mutation, which arises *de novo* in the HDR patient (Fig. 2) is unusual in being in this class, particularly as three nearby truncating mutations involving codons 351, 355 and 367, which leave the ZnF2 intact, have been reported to result in a loss of DNA binding and thereby belong to the first class (13). These mutations, which are located in the basic region result in the loss or partial loss of the conserved QTRNRK motif, which, in GATA1 has been shown to be vital for high affinity recognition of the GATA motif (26,31) and is found in the region of the GATA protein that lies in the DNA minor groove. As this motif is absolutely conserved in GATA3, it seems highly probable that it plays the same role in GATA3 (Fig. 5). The Leu348Arg mutant, however, does not disrupt this domain, and the affinity of binding of this mutant GATA3 molecule is unimpaired (Fig. 4). In contrast, Leu348 is found at the end of an α-helix linking ZnF2 and the C-terminal basic domain; ZnF2 makes contact with the DNA in the major groove whereas the C-terminal basic domain makes contact with the DNA minor groove (31) (Fig. 5). Hence, the Leu348 residue lies within

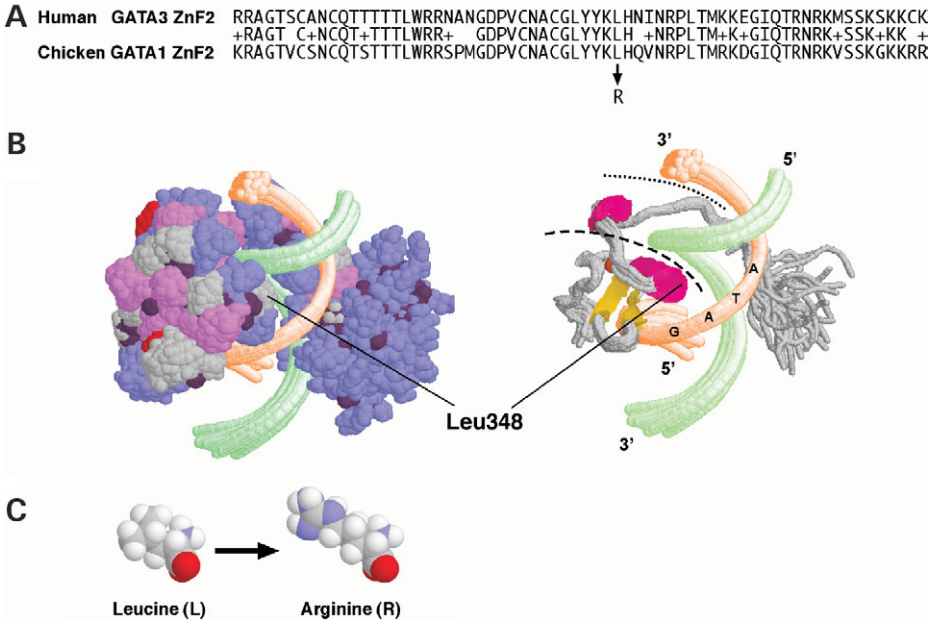

Figure 5. Three-dimensional structure of the human GATA3-ZnF2 based on the chicken GATA1 ZnF2. Human GATA3, which consists of 444 amino acids and human GATA1, which consists of 413 amino acids, belong to the same subfamily (11) and share structural similarities that include two ZnFs (Fig. 1) and a basic amino region that is located C-terminally and adjacent to ZnF2 (13). (**A**) Human GATA3-ZnF2 (residues 318 to 343) and its adjacent C-terminal region (residues 344 to 378) has 78% identity and 93% similarity to the chicken GATA1-ZnF2 (residues 164 to 189) and the adjacent C-terminal region (residues 190 to 224). The conserved QTRNRK motif, which has been shown to be important for high affinity recognition of the GATA motif (26,31), is underlined. (**B**) The three-dimensional structure of chicken GATA1-ZnF2 and the adjacent C-terminal region has been characterized (31), thereby enabling us to use this to construct a three-dimensional model of hGATA3-ZnF2 and its adjacent basic amino-acid region. The backbone is shown in *dark magenta*; hydrophobic side chains as grey; polar side chains as *magenta*; acidic side chains as *red*; and basic side chains as *blue*. The antiparallel DNA strands are shown in orange and green, with the G, A, T and A nucleosides shown. The Leu 348 residue lies at the end of an α-helix *(red)* which resides within the DNA major groove (dashed line), and makes contact with DNA at the point where the GATA motif is found. (**C**) The Leu 348 mutation results in the substitution of a non-polar hydrophobic Leu residue for a positively charged larger Arg residue, and this is likely to affect conformational changes in the DNA double helix and thereby alter transcriptional activity. The minor groove is indicated by the dotted line. The color scheme derives from the Corey, Pauling, Koltun (CPK) color scheme as follows: Hydrophobic = carbon; acidic = oxygen; basic = nitrogen; polar but uncharged = a mixture of oxygen *(red)* and nitrogen *(blue)*, namely *magenta* and beta strands are shown in yellow.

Table 3. HDR clinical findings and GATA3 mutations

	HDR phenotypes[a]				Total
	HDR	HD	HR	H only	
GATA3 mutation[b]					
Y	27	13	0	0	40
N	2	7	0	14	23
Total	29	20	0	14	63

[a]H, hypoparathyroidism; D, deafness; R, renal abnormalities.
[b]GATA3 mutation: Y, yes; N, none detected.
χ^2 test: $P < 0.001$, with three degrees of freedom.

the DNA major groove and makes contact with DNA at the point where the GATA motif is found. Within the major groove, the specific interactions that occur between GATA1 and DNA have been shown by solution nuclear magnetic resonance (NMR) studies (26) to be mainly hydrophobic in nature. Thus, the replacement of the non-polar leucine residue with the larger polar arginine residue might have been predicted to have a significant effect on DNA binding, particularly as the linker section between ZnF2 and the QTRNRK motif is not in itself sufficient for DNA binding (26). However, our results show that the Leu348Arg mutation has no effect on the affinity of DNA binding (Fig. 4) and the mechanism may possibly involve a conformational change. For example, GATA1 bends DNA upon binding (32) and solution NMR studies of the C-terminal finger of GATA1 have shown that binding to its cognate DNA sequence results in bending of the DNA by an overall angle of about 15° (31). This kink probably results from the insertion of the C-terminal basic residues required for DNA binding (25,26) into the minor groove. Thus, the Leu348Arg mutation may affect the conformational changes that GATA3 binding induces in the DNA helix and is likely to impair efficient transcription from GATA3 regulated genes important in parathyroid, kidney and inner ear development. These results expand the spectrum of HDR associated GATA3 mutations and also increase our understanding of mechanisms by which GATA3 mutations cause the HDR syndrome.

MATERIALS AND METHODS

Patients

Thirty-eight individuals (15 males and 23 females) from 21 unrelated families with HDR were ascertained. The families were from Europe, North America, Turkey, Israel and Australia. Twenty-nine individuals (10 males and 19 females) were affected with HDR and nine individuals (five males and four

females) were unaffected. All of the 29 affected individuals had hypoparathyroidism with serum calcium ranging from 1.04 to 2.15 mmol/L, and this was associated with tetany or seizures in 18 patients, but was asymptomatic in 11 patients (Table 1). Bilateral sensorineural deafness was found in 24 patients (eight males and 16 females) with the age at diagnosis ranging from at birth to 38 years. Renal abnormalities were found in 15 patients (four males and 11 females), of whom seven had hypoplastic kidneys, two had unilateral renal agenesis and two had developed end-stage renal failure. Fourteen patients (10 males and four females) with childhood onset of isolated hypoparathyroidism (clinical data not shown) were also ascertained; six of these patients had a history of familial isolated hypoparathyroidism.

DNA sequence analysis of the *GATA3* gene

Venous blood was obtained after informed consent, as approved by the local ethical committee, and used to extract leukocyte DNA (13). Nine pairs of *GATA3* specific primers were used for polymerase chain reaction (PCR) amplification of the six exons and 10 intron–exon boundaries using 50 ng of genomic DNA as described (13). The DNA sequences of both strands were determined by *Taq* polymerase cycle sequencing and resolved on a semi-automated detection system (ABI 377XL sequencer, Applied Biosystems, Foster City, CA, USA) (13). DNA sequence abnormalities, which were confirmed by restriction endonuclease analysis or by repeat sequence analysis, were demonstrated to be absent in the DNA obtained from 55 unaffected unrelated individuals, using methods previously described (13).

Reverse transcriptase–polymerase chain reaction (RT–PCR) studies

RT–PCR was utilized to investigate mRNA splicing abnormalities, using total RNA extracted from EBV-transformed lymphoblastoid cell lines from the proband of family 8/05 (Tables 1 and 2) and an unrelated normal individual, as previously described (13,23). RT–PCR was performed using *GATA3*-specific primers; the forward and reverse primers consisted of the sequences: 5′ AGATGGCACGGGACACTACC 3′ (nucleotides 831 to 850 in exon 4); and 5′ GAGCTGTTCTTGGGGAAGTCC 3′ (nucleotides 1152 to 1172 in exon 6), respectively. The DNA sequences of the purified RT–PCR products were then determined using methods previously reported (13,33).

Protein preparation and EMSAs

COS-7 cells, which do not endogenously express GATA3, were transfected using lipofectAMINE Plus (Invitrogen, Carlsbad, CA, USA) with either a wild-type GATA3 construct prepared in pcDNA3.1 (GATA3-pcDNA3) (Invitrogen) or a construct harboring the mutation that was introduced by the use of site-directed mutagenesis (QuikChange, Stratagene, La Jolla, CA, USA), as previously described (3,13). Forty eight hours post-transfection, the cells were harvested, lysed and fractionated into nuclear and cytoplasmic extracts using NE-PER kit (Pierce). Western blot analysis using the HG3-31 monoclonal antibody against GATA3 (Santa Cruz Biotechnology Inc., Santa Cruz, CA, USA) was used to detect the presence of GATA3 protein in the cell fractions (13). Antibodies against lamin and α-tubulin were used to assess the quality of the subcellular fraction preparations. Nuclear protein extracts (5 μg) were used in binding reactions that utilized a ^{32}P-labeled double-stranded oligonucleotide that contained GATA3 consensus sequences (5′-cacttg*ata*acagaaagt*gata*actct) or mutated sequences (5′-cacttc*tata*acagaaagt*ctta*aactct). The binding reactions were resolved by non-denaturing 4% polyacrylamide gel electrophoresis (PAGE). For dissociation shift assays, unlabeled competitor DNA was added to a 100-fold excess to the binding reactions, and aliquots were removed after 0, 10, 30 and 60 min for non-denaturing PAGE (34,35). To confirm the presence of GATA3 in the complex, a supershift assay with GATA3 antibody was performed (36).

Computer modeling of GATA3 ZnF2 structure

The evolutionary conservation of GATA3 residues and their homologies between other GATA factors were examined by using an online multiple sequence alignment (Clustal W, http://www.ebi.ac.uk/clustalw/). The sequence data were obtained from the NCBI database (http://www.ncbi.nlm.nih.gov/). The three-dimensional NMR structure of chicken GATA1 ZnF2 has been reported (37), and because the C-terminal fingers of GATA1 and GATA3 are over 80% identical and have more than 90% similarity, we modeled the position of the GATA3 mutant Leu348Arg, identified in the proband from family 8.2/04 (Table 2), on this framework. The three-dimensional structure of GATA1 C-terminal is archived in the Protein Data Bank at the European Bioinformatics Institute, (http://rutgers.rcsb.org/pdb/index.html) with the accession number 3GAT and this was visualized using the Chime program (MDL Information Systems Inc., San Leandro, CA, USA) as described (13).

Statistical analysis

The HDR phenotype data from this study were pooled with those of our three previous studies (3,13,15) from which detailed clinical information was available, to undertake an analysis of an association between the phenotypes and the presence or absence of *GATA3* mutations. Statistical analysis that utilized the χ^2 test was performed using the Georgetown Linguistics Chi Square Tutorial (http://www.georgetown.edu/faculty/ballc/webtools/web_chi_tut.html) as previously described (38,39).

ACKNOWLEDGEMENTS

We thank M.-C. Vantyghem, E.A. Cummings, C. Regis, N. Philip, G. Standaert, D. Vincent and D. Zimmerman for providing access to patients and clinical information. This work was supported by the UK Medical Research Council (to A.A., P.T.C., I.V.G., B.H., M.A.N. and R.V.T.). A.A. is a Medical Research Council Training Fellow and I.V.G. is a Medical Research Council PhD student.

Conflict of Interest statement. None declared.

REFERENCES

1. Marx, S.J. (2000) Hyperparathyroid and hypoparathyroid disorders. *N. Engl. J. Med.*, **343**, 1863–1875.
2. Thakker, R.V. (2001) Genetic developments in hypoparathyroidism. *Lancet*, **357**, 974–976.
3. Van Esch, H., Groenen, P., Nesbit, M.A., Schuffenhauer, S., Lichtner, P., Vanderlinden, G., Harding, B., Beetz, R., Bilous, R.W., Holdaway, I. *et al*. (2000) GATA3 haplo-insufficiency causes human HDR syndrome. *Nature*, **406**, 419–422.
4. Bilous, R.W., Murty, G., Parkinson, D.B., Thakker, R.V., Coulthard, M.G., Burn, J., Mathias, D. and Kendall-Taylor, P. (1992) Autosomal dominant familial hypoparathyroidism, sensorineural deafness, and renal dysplasia. *N. Engl. J. Med.*, **327**, 1069–1074.
5. Diaz, G.A., Gelb, B.D., Ali, F., Sakati, N., Sanjad, S., Meyer, B.F. and Kambouris, M. (1999) Sanjad-Sakati and autosomal recessive Kenny–Caffey syndromes are allelic: evidence for an ancestral founder mutation and locus refinement. *Am. J. Med. Genet.*, **85**, 48–52.
6. Ding, C., Buckingham, B. and Levine, M.A. (2001) Familial isolated hypoparathyroidism caused by a mutation in the gene for the transcription factor GCMB. *J. Clin. Invest.*, **108**, 1215–1220.
7. Bowl, M.R., Nesbit, M.A., Harding, B., Levy, E., Jefferson, A., Volpi, E., Rizzoti, K., Lovell-Badge, R., Schlessinger, D., Whyte, M.P.6. (2005) An interstitial deletion–insertion involving chromosomes 2p25.3 and Xq27.1, near SOX3, causes X-linked recessive hypoparathyroidism. *J. Clin. Invest.*, **115**, 2822–2831.
8. de la Chapelle, A., Herva, R., Koivisto, M. and Aula, P. (1981) A deletion in chromosome 22 can cause DiGeorge syndrome. *Hum. Genet.*, **57**, 253–256.
9. Yagi, H., Furutani, Y., Hamada, H., Sasaki, T., Asakawa, S., Minoshima, S., Ichida, F., Joo, K., Kimura, M., Imamura, S. *et al*. (2003) Role of TBX1 in human del22q11.2 syndrome. *Lancet*, **362**, 1366–1373.
10. Parvari, R., Hershkovitz, E., Grossman, N., Gorodischer, R., Loeys, B., Zecic, A., Mortier, G., Gregory, S., Sharony, R., Kambouris, M. *et al*. (2002) Mutation of TBCE causes hypoparathyroidism-retardation-dysmorphism and autosomal recessive Kenny–Caffey syndrome. *Nat. Genet.*, **32**, 448–452.
11. Orkin, S.H. (1992) GATA-binding transcription factors in hematopoietic cells. *Blood*, **80**, 575–581.
12. Tevosian, S.G., Deconinck, A.E., Cantor, A.B., Rieff, H.I., Fujiwara, Y., Corfas, G. and Orkin, S.H. (1999) FOG-2: a novel GATA-family cofactor related to multitype zinc-finger proteins Friend of GATA-1 and U-shaped. *Proc. Natl. Acad. Sci. USA*, **96**, 950–955.
13. Nesbit, M.A., Bowl, M.R., Harding, B., Ali, A., Ayala, A., Crowe, C., Dobbie, A., Hampson, G., Holdaway, I., Levine, M.A. *et al*. (2004) Characterization of GATA3 mutations in the hypoparathyroidism, deafness, and renal dysplasia (HDR) syndrome. *J. Biol. Chem.*, **279**, 22624–22634.
14. Muroya, K., Hasegawa, T., Ito, Y., Nagai, T., Isotani, H., Iwata, Y., Yamamoto, K., Fujimoto, S., Seishu, S., Fukushima, Y. *et al*. (2001) GATA3 abnormalities and the phenotypic spectrum of HDR syndrome. *J. Med. Genet.*, **38**, 374–380.
15. Zahirieh, A., Nesbit, M.A., Ali, A., Wang, K., He, N., Stangou, M., Bamichas, G., Sombolos, K., Thakker, R.V. and Pei, Y. (2005) Functional analysis of a novel GATA3 mutation in a family with the hypoparathyroidism, deafness, and renal dysplasia syndrome. *J. Clin. Endocrinol. Metab.*, **90**, 2445–2450.
16. Mino, Y., Kuwahara, T., Mannami, T., Shioji, K., Ono, K. and Iwai, N. (2005) Identification of a novel insertion mutation in GATA3 with HDR syndrome. *Clin. Exp. Nephrol.*, **9**, 58–61.
17. Adachi, M., Tachibana, K., Asakura, Y. and Tsuchiya, T. (2006) A novel mutation in the GATA3 gene in a family with HDR syndrome (Hypoparathyroidism, sensorineural Deafness and Renal anomaly syndrome). *J. Pediatr. Endocrinol. Metab.*, **19**, 87–92.
18. Chiu, W.Y., Chen, H.W., Chao, H.W., Yann, L.T. and Tsai, K.S. (2006) Identification of three novel mutations in the GATA3 gene responsible for familial hypoparathyroidism and deafness in the Chinese population. *J. Clin Endocrinol. Metab.*, **91**, 4587–4592.
19. Fox, A.H., Kowalski, K., King, G.F., Mackay, J.P. and Crossley, M. (1998) Key residues characteristic of GATA N-fingers are recognized by FOG. *J. Biol. Chem.*, **273**, 33595–33603.
20. Krawczak, M., Reiss, J. and Cooper, D.N. (1992) The mutational spectrum of single base-pair substitutions in mRNA splice junctions of human genes: causes and consequences. *Hum. Genet.*, **90**, 41–54.
21. Christie, P.T., Harding, B., Nesbit, M.A., Whyte, M.P. and Thakker, R.V. (2001) X-linked hypophosphatemia attributable to pseudoexons of the PHEX gene. *J. Clin. Endocrinol. Metab.*, **86**, 3840–3844.
22. Lemos, M.C., Kotanko, P., Christie, P.T., Harding, B., Javor, T., Smith, C., Eastell, R. and Thakker, R.V. (2005) A novel EXT1 splice site mutation in a kindred with hereditary multiple exostosis and osteoporosis. *J. Clin. Endocrinol. Metab.*, **90**, 5386–5392.
23. Parkinson, D.B. and Thakker, R.V. (1992) A donor splice site mutation in the parathyroid hormone gene is associated with autosomal recessive hypoparathyroidism. *Nat. Genet.*, **1**, 149–152.
24. Mount, S.M. (1982) A catalogue of splice junction sequences. *Nucleic. Acids Res.*, **10**, 459–472.
25. Yang, H.Y. and Evans, T. (1993) Distinct roles for the two cGATA-1 finger domains. *Mol. Cell. Biol.*, **12**, 4562–4570.
26. Omichinski, J.G., Trainor, C., Evans, T., Gronenborn, A.M., Clore, G.M. and Felsenfeld, G. (1993) A small single-'finger' peptide from the erythroid transcription factor GATA-1 binds specifically to DNA as a zinc or iron complex. *Proc. Natl. Acad. Sci. USA*, **90**, 1676–1680.
27. Petersen, M.B. and Willems, P.J. (2006) Non-syndromic, autosomal-recessive deafness. *Clin. Genet.*, **69**, 371–392.
28. Bitner-Glindzicz, M. (2002) Hereditary deafness and phenotyping in humans. *Br. Med. Bull.*, **63**, 73–94.
29. Porteous, S., Torban, E., Cho, N.P., Cunliffe, H., Chua, L., McNoe, L., Ward, T., Souza, C., Gus, P., Giugliani, R. *et al*. (2000) Primary renal hypoplasia in humans and mice with PAX2 mutations: evidence of increased apoptosis in fetal kidneys of Pax2(1Neu) +/− mutant mice. *Hum. Mol. Genet.*, **9**, 1–11.
30. Schonfelder, E.M., Knuppel, T., Tasic, V., Miljkovic, P., Konrad, M., Wuhl, E., Antignac, C., Bakkaloglu, A., Schaefer, F., Weber, S. and ESCAPE Trial Group (2006) Mutations in Uroplakin IIIA are a rare cause of renal hypodysplasia in humans. *Am. J. Kidney Dis.*, **47**, 1004–1012.
31. Omichinski, J.G., Clore, G.M., Schaad, O., Felsenfeld, G., Trainor, C., Appella, E., Stahl, S.J. and Gronenborn, A.M. (1993) NMR structure of a specific DNA complex of Zn-containing DNA binding domain of GATA-1. *Science*, **261**, 438–446.
32. Schwartzbauer, G., Schlesinger, K. and Evans, T. (1992) Interaction of the erythroid transcription factor cGATA-1 with a critical auto-regulatory element. *Nucleic Acids Res.*, **20**, 4429–4436.
33. Lloyd, S.E., Pearce, S.H., Fisher, S.E., Steinmeyer, K., Schwappach, B., Scheinman, S.J., Harding, B., Bolino, A., Devoto, M., Goodyer, P. *et al*. (1996) A common molecular basis for three inherited kidney stone diseases. *Nature*, **379**, 445–449.
34. Nichols, K.E., Crispino, J.D., Poncz, M., White, J.G., Orkin, S.H., Maris, J.M. and Weiss, M.J. (2000) Familial dyserythropoietic anaemia and thrombocytopenia due to an inherited mutation in GATA1. *Nat. Genet.*, **24**, 266–270.
35. Trainor, C.D., Ghirlando, R. and Simpson, M.A. (2000) GATA zinc finger interactions modulate DNA binding and transactivation. *J. Biol. Chem.*, **275**, 28157–28166.
36. Dame, C., Sola, M.C., Lim, K.C., Leach, K.M., Fandrey, J., Ma, Y., Knopfle, G., Engel, J.D. and Bungert, J. (2004) Hepatic erythropoietin gene regulation by GATA-4. *J. Biol. Chem.*, **279**, 2955–2961.
37. Tjandra, N., Omichinski, J.G., Gronenborn, A.M., Clore, G.M. and Bax, A. (1997) Use of dipolar 1H-15N and 1H-13C couplings in the structure determination of magnetically oriented macromolecules in solution. *Nat. Struct. Biol.*, **4**, 732–738.
38. Crossey, P.A., Richards, F.M., Foster, K., Green, J.S., Prowse, A., Latif, F., Lerman, M.I., Zbar, B., Affara, N.A., Ferguson-Smith, M.A. *et al*. (1994) Identification of intragenic mutations in the von Hippel-Lindau disease tumour suppressor gene and correlation with disease phenotype. *Hum. Mol. Genet.*, **3**, 1303–1308.
39. Pannett, A.A., Kennedy, A.M., Turner, J.J., Forbes, S.A., Cavaco, B.M., Bassett, J.H., Cianferotti, L., Harding, B., Shine, B., Flinter, F. *et al*. (2003) Multiple endocrine neoplasia type 1 (MEN1) germline mutations in familial isolated primary hyperparathyroidism. *Clin. Endocrinol. (Oxf.)*, **58**, 639–646.
40. Burset, M., Seledtsov, I.A. and Solovyev, V.V. (2001) SpliceDB: database of canonical and non-canonical mammalian splice sites. *Nucleic. Acids Res.*, **29**, 255–259.